

## Characterization of aluminum-based coatings after short term exposure during irradiation campaign in the LVR-15 fission reactor

Roman Petráš<sup>a</sup>, Klára Kunzová<sup>a,\*</sup>, Alica Fedoriková<sup>a</sup>, Jaroslav Kekrt<sup>a</sup>, Michal Kordač<sup>a</sup>, Fabio Di Fonzo<sup>b</sup>, Boris Paladino<sup>b</sup>, Carsten Schroer<sup>c</sup>, Julia Lorenz<sup>c</sup>, Marco Utili<sup>d</sup>, Ladislav Vála<sup>a</sup>

<sup>a</sup> Centrum výzkumu Řež (CVR), Hlavní 130, 250 68, Husinec - Řež, Czech Republic

<sup>b</sup> Centre for Nano Science and Technology @PoLiMi, Istituto Italiano di Tecnologia, Via Pascoli 70/3, 20133, Milano, Italy

<sup>c</sup> Karlsruhe Institute of Technology (KIT), Hermann-von-Helmholtz Platz 1, 76344 Eggenstein-Leopoldshafen, Germany

<sup>d</sup> ENEA Brasimone, 40032, Camugnano, Bologna, Italy

### ARTICLE INFO

#### Keywords:

Eurofer97  
Pb-16Li  
Aluminum-based coating  
PLD techniques  
ECX techniques  
Cross-section analysis

### ABSTRACT

Protective aluminum-based coatings represent a promising anti-permeation and anti-corrosion barrier for breeding blanket systems developed for European DEMO fusion reactor. Following the prior in-depth characterizations, selected coating candidates were subjected to a combined test consisting of contact with liquid Pb-16Li, its repeated in-situ solidification and re-melting, tritium permeation during gamma and neutron irradiation in the LVR-15 fission reactor. During the sample exposure in the reactor, the temperature of Pb-16Li was between 300 and 425 °C. The irradiation damage averaged over the sample volume estimated by FISPACT code was limited to 0.037 dpa. This article presents post-irradiation characterization of cylindrical Eurofer97 samples coated by electro-chemical X-metal deposition from ionic liquid (ECX) and pulsed laser deposition (PLD) techniques. The coating damage relative to a reference uncoated sample is discussed.

### 1. Introduction

In the framework of the EUROfusion project, four different Breeding Blanket concepts for European DEMO fusion reactor are being developed [1]. Three of them, WCLL (Water-cooled lithium-lead), HCLL (Helium-cooled lithium-lead) and DCLL (Dual coolant lithium-lead), are based on use of liquid metal breeder Pb-16Li [2,3]. Reduced activation ferritic-martensitic (RAFM) steel Eurofer97 represents a structural material employed for breeding blanket designs within the EUROfusion project [4]. The interaction between the material and flowing Pb-16Li breeder entails corrosion damage, whereas loss of produced tritium that permeates through the wall of the blanket components is inherent to the use of steel. Protective aluminum-based coating is being developed to mitigate the two effects; their physical properties have been investigated within the EUROfusion project. The techniques developed for production of Al-based coatings and their deposition on the Eurofer97 steel are electrochemical X-metal deposition from ionic liquid (ECX) [5–7] and pulsed laser deposition (PLD) [8,9]. As for the ECX coating, the formation of surface oxides, including Al<sub>2</sub>O<sub>3</sub> considered most effective as to both the reduction of tritium permeation and corrosion

resistance, is facilitated by performing the necessary heat treatments (after electroplating Al) in flowing technical argon with residual oxygen. In contrast, PLD works with direct Al<sub>2</sub>O<sub>3</sub> deposition. Previously, comprehensive tests have been carried out to assess separately the properties of coatings produced by different techniques in terms of their adhesion on Eurofer97 steel, compatibility with liquid metal Pb-16Li under breeding blanket operational conditions, thermal cycling, hydrogen and deuterium permeation reduction factor, ion irradiation resistance and so on [6,10–12].

The aim of this paper is to report on the state of the selected candidate coatings after a combined effect involving exposure of the coatings to a liquid Pb-16Li under neutron and gamma irradiation in the LVR-15 fission reactor, thermal cycling including in-situ freezing and melting of the Pb-16Li alloy as well as tritium permeation across the coated wall of the sample during tritium permeation experiment.

\* Corresponding author.

E-mail address: [klara.kunzova@cvrez.cz](mailto:klara.kunzova@cvrez.cz) (K. Kunzová).

<https://doi.org/10.1016/j.fusengdes.2021.112521>

Received 27 November 2020; Received in revised form 16 February 2021; Accepted 19 March 2021

Available online 2 April 2021

0920-3796/© 2021 The Authors.

Published by Elsevier B.V. This is an open access article under the CC BY-NC-ND license

(<http://creativecommons.org/licenses/by-nc-nd/4.0/>).

## 2. Material, coatings and experimental setup

### 2.1. Material investigated

Eurofer97 samples in the form of closed tubes were produced in ENEA based on the CVR requirements; the sample geometry is shown in Fig. 1. The diameter of the samples was 10 mm with a wall thickness of 1 mm. The chemical composition of Eurofer97 can be found elsewhere [13]. Subsequently, samples were provided with a Fe-Al diffusion coating by the ECX technique [6,12] and Al<sub>2</sub>O<sub>3</sub> coatings by the PLD technique [9,14,15] at KIT and IIT, respectively. The thickness of the individual coatings is given in Table 1.

### 2.2. Experimental setup

Following the design given in [16], a PbLi irradiation capsule made of 1.4404 (AISI 316 L) was manufactured in CVR. The overall dimensions of the capsule were 225 mm in length and 48 mm in diameter. The irradiation capsule is schematically shown in Fig. 2. The capsule was equipped with thermocouples at three locations at 5, 80 and 160 mm from the bottom of the capsule. The thermocouples were a multi element temperature probes with 5 K-type sensors in a single sheath made from 1.4571. Three of the sensors allowed measurement of the vertical temperature profile of Pb-16Li (at the bottom, middle and top) with the other two monitoring temperature of the capsule in the region above the Pb-16Li level. Temperature is then adjusted with a dedicated temperature control and heat removal system based on regulation of gas concentration in the gas gap of the irradiation device as described in [16].

Four samples (Fig. 1, Table 1) were placed symmetrically along the axis. Before installing the irradiation capsule into the reactor, it was filled with 1774 g of Pb-16Li, which level was ~10 mm below the lid of the capsule. The eutectic Pb-16Li alloy (technical grade) was prepared by CAMEX company as a batch no. 3N8-06/14; it had initial Pb purity of 99.98 % containing 150 ppm of Bi and natural Li containing 7.6 % of <sup>6</sup>Li and 92.4 % of <sup>7</sup>Li isotopes.

The PbLi capsule was placed in the LVR-15 fission reactor for a 620 h long irradiation campaign. Since the main goal of the experiment in the reactor was to study the permeation of tritium through the samples and to estimate experimentally the PRF (Permeation Reduction Factor), only one irradiation campaign was carried out. Therefore, the irradiation damage averaged over the sample volume estimated using FISPACT code is only 0.037 dpa for the reactor campaign. Temperature of Pb-16Li in the capsule was maintained above 300 °C, i.e. close to and above the operation Pb-16Li temperature of the WCLL and HCLL blankets [3] and in the temperature operation range of the DCLL blanket [17]. The Pb-16Li temperature measured along the PbLi capsule varied from 300 °C at the bottom of the capsule to 425 °C at the upper level of liquid metal. For this temperature range, given geometry of the capsule and the actual position in the reactor core, the maximum Pb-16Li velocity was estimated to be 2.9 cm/s and the average velocity along the samples was 1 cm/s. The natural circulation of molten Pb-16Li driven by the temperature gradient was promoted by a field tube which thermally separated the cooling zone at the level of the outer wall of the capsule from the central region, where gamma-ray heating of the Pb-16Li alloy

**Table 1**

List of the samples.

| Sample No. | Type of the coating | Coating thickness [μm] |
|------------|---------------------|------------------------|
| 1          | Reference           | 0                      |
| 2          | ECX                 | 40–70*                 |
| 3          | PLD                 | 3                      |
| 4          | PLD                 | 5                      |

\* Thickness of diffusion layer.

prevails. Additionally, the campaign included 11 reactor shutdowns for short-term maintenance, typically in duration of 1.5 h, during which the PbLi capsule temperature decreased down to 40 °C causing in consequence 11 thermal cycles including solidification and melting of Pb-16Li inside the capsule. After the irradiation campaign, the samples were extracted from the PbLi capsule in the CVR hot cells and prepared for the subsequent post irradiation analyses.

The sample surface was not treated in terms of chemical cleansing to avoid possible damage of the surface. Transversal cross-sections were prepared from the locations indicated in Fig. 2 to verify the surface state after the experiment. For microstructure and chemical analysis, SEM Tescan MIRA 3 was used. SEM is installed in semi-hot cell with auto-emission cathode Field Emission Gun (FEG) working with acceleration voltage 0.05–30 kV. The SEM is equipped with detector X-MaxN for Energy Dispersive X-ray analysis (EDX). All operations relating to post irradiation analyses were conducted remotely because of high activity of the samples (each sample had presented activity about 24 mS/h).

## 3. Results

### 3.1. Uncoated reference samples

Cross-sections of the pristine Eurofer97 sample after exposure in the PbLi irradiation capsule are documented in Fig. 3. The common aspect of sample exposure to liquid Pb-16Li environment is formation of rough surface formed by residual Pb-16Li (bright overlay in Fig. 3). Detailed inspection of the interface between the material and Pb-16Li layer revealed an important attribute identified in terms of surface roughness; the roughness of the sample surface exposed to higher temperature was typically more pronounced.

The EDS-line scan analysis of the pristine Eurofer97 is documented in Fig. 4. A slight depletion of Cr got gradually pronounced in the proximity of sample surface. Nevertheless, the thickness of the depleted zone is smaller than the spatial resolution of the EDX line scan.

### 3.2. Samples with ECX coating

Fig. 5 shows cross-sections of the Eurofer97 sample coated by the ECX technique after exposure in the PbLi irradiation capsule. It has been observed that the surface relief is characterized by high roughness. The surface roughness is temperature related and more pronounced on the part of the sample exposed to higher temperature. Small capillary cracks on the sample surface along with pores of different size in the material volume can be recognized.

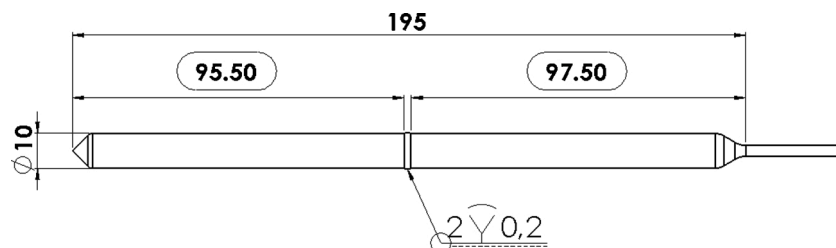


**Fig. 1.** Eurofer97 samples for testing the coatings (dimensions in mm).

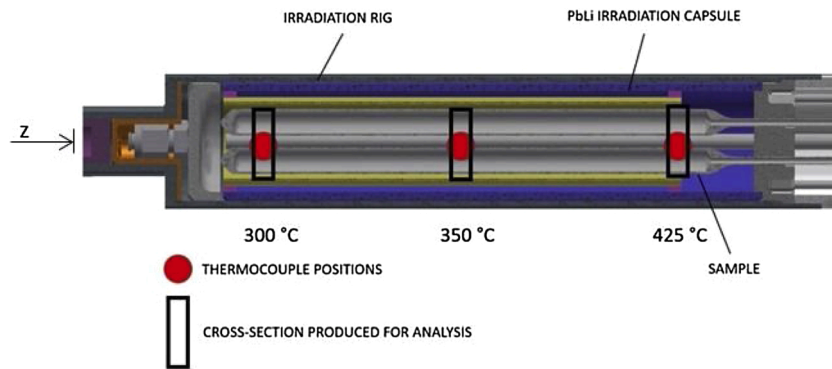


Fig. 2. A cross section view of the PbLi capsule; the red dots indicate thermocouple positions and rectangles indicate the locations of cross-sections exposed to investigation by means of SEM and EDS technique (For interpretation of the references to colour in this figure legend, the reader is referred to the web version of this article).

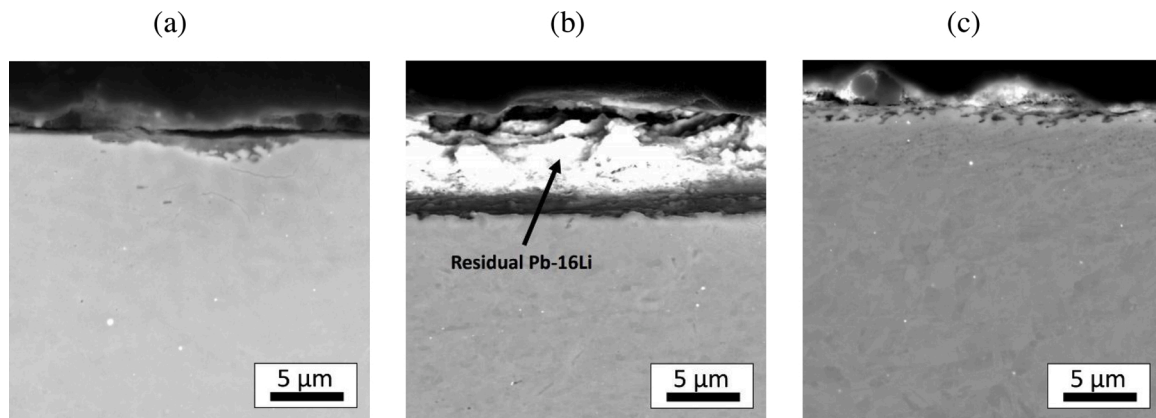


Fig. 3. Cross-section micrographs of the uncoated sample. Different locations along the sample tubes are shown with respective temperature of the exposure (a) 300 °C (b) 350 °C (c) 425 °C.

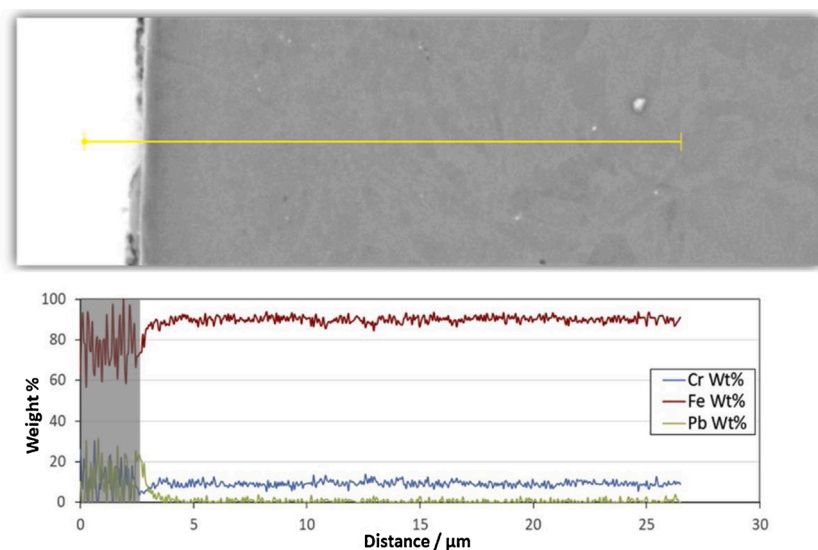


Fig. 4. Line scan of chemical composition of uncoated sample, location exposed at 425 °C. The signal captured from the resin is marked as a grey region.

Fig. 6 shows the EDS-line scan analysis of the ECX coated Eurofer97 sample. The Fe-Al layer consists of two sub-layers easily identified from the profile of Al content. While the content of Al in the outer layer is typically almost constant over approx. 10 μm, the diffusion layer is distinguished by the gradual decrease in Al content, which is detected

over a thickness of approx. 70 μm, as shown in Fig. 6. Similarly, a slight decrease in Cr content towards the sample surface can be recognized within the diffusion layer. Moreover, the interface between the outer and the diffusion layer is decorated by large pores. Comparing to large pores located preferentially at the interface between the layers, small

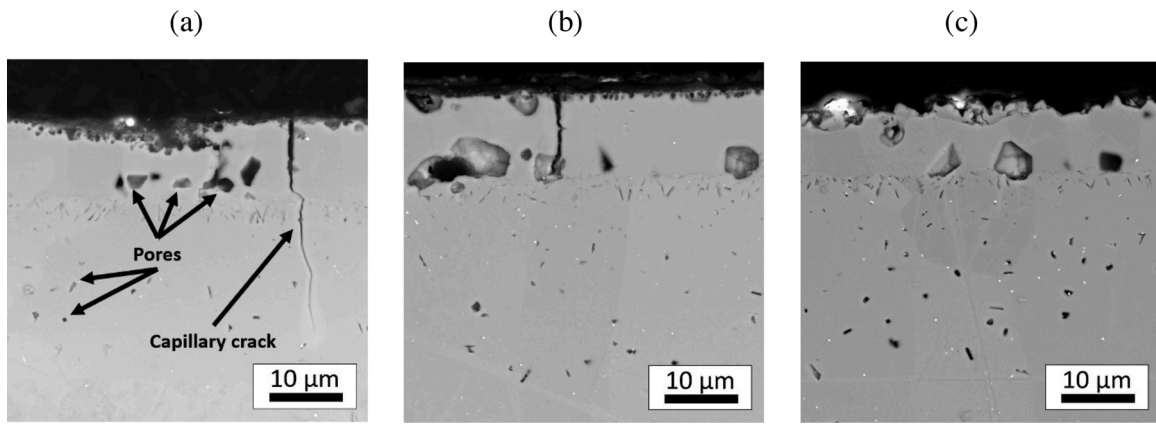


Fig. 5. Cross-section micrographs of the sample with ECX coating. Different locations along the sample tube are shown with respective temperature of the exposure (a) 300 °C (b) 350 °C (c) 425 °C.

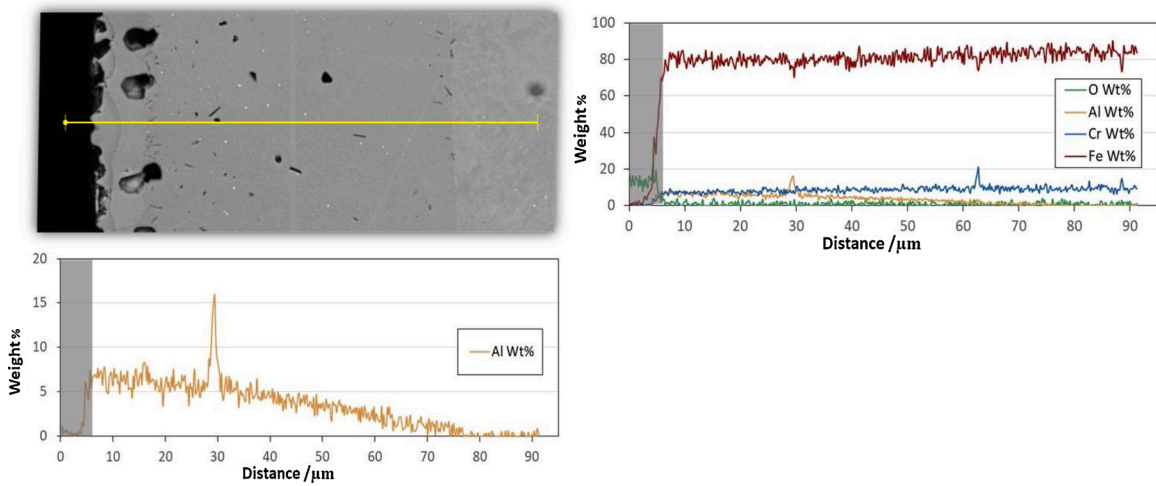


Fig. 6. Line scan of chemical composition of ECX coated sample. The signal captured from the resin is marked as a grey region.

pores are distributed within the diffusion layer (see Fig. 5(c)).

### 3.3. Samples with PLD coating

Cross-sections of Eurofer97 samples coated by PLD technique having thickness of 3 or 5 μm after exposure in the PbLi irradiation capsule are reported in Figs. 7 and 8, respectively. Both coating barriers studied

were found to be smooth and free of cracks in all the cross-sections investigated. No damage of the coatings related to the exposure in the PbLi capsule was observed. The investigation of the cross-sections did not show any loss of adhesion or delamination effects at the coating-Eurofer97 interface.

The performed EDS line-scan shows presence of Al and O corresponding to Al<sub>2</sub>O<sub>3</sub> layer deposited by the PLD technique on the pristine

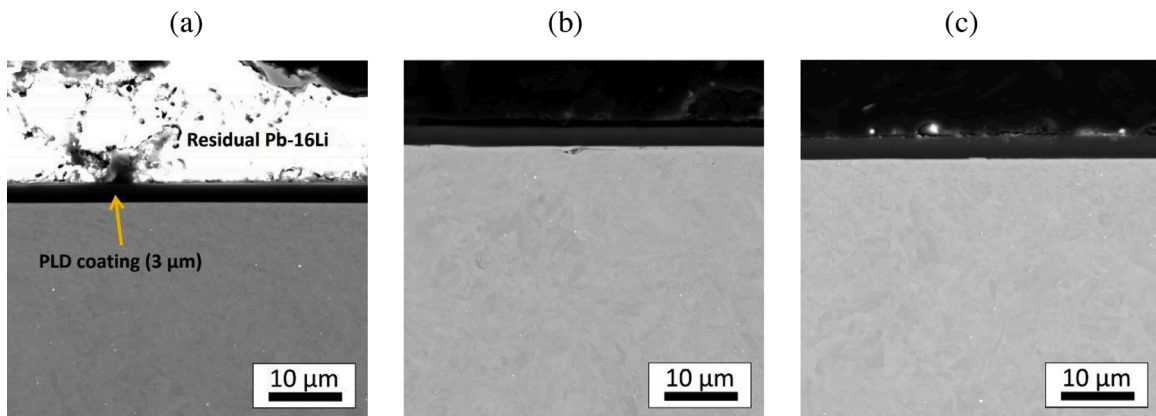


Fig. 7. Cross-section micrographs of the sample with PLD coating thickness of 3 μm. Different location along the sample tube are shown with respective temperature of the exposure (a) 300 °C (b) 350 °C (c) 425 °C.



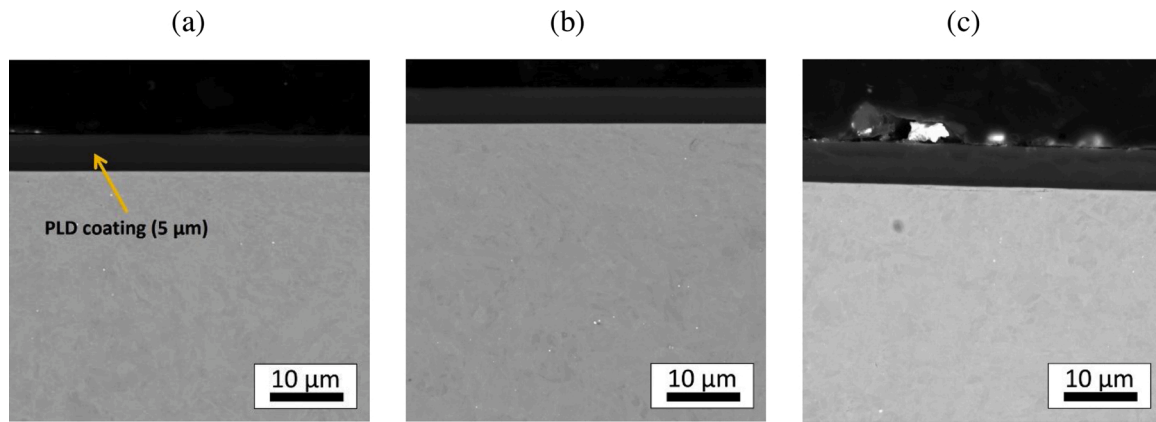


Fig. 8. Cross-section micrographs of the sample with PLD coating thickness of 5  $\mu\text{m}$ . Different locations along the sample tube are shown with respective temperature of the exposure (a) 300  $^{\circ}\text{C}$  (b) 350  $^{\circ}\text{C}$  (c) 425  $^{\circ}\text{C}$ .

Eurofer97 showing no change in its chemical composition after the reactor campaign, as shown in Fig. 9.

#### 4. Discussion

The paper reports on the evaluation of the sample surfaces after a synergic effect of liquid Pb-16Li, neutron and gamma irradiation, thermal cycling and in-situ freezing and melting of liquid metal.

SEM cross-section inspection of uncoated sample reveals surface roughness which is more pronounced with increasing temperature. Pronounced surface roughness is typical for exposure of Eurofer97 to the Pb-16Li environment [18]. The exposure of a bare material to Pb-16Li at 550  $^{\circ}\text{C}$  for 2000, 4000 and 8000 h resulted in corrosion attack forming porous structure. The corrosion attack was found to be enhanced by fluid flow reaching up to 400  $\mu\text{m}/\text{year}$  at a flow velocity of 0.22 m/s [19]. In the present experimental setup, the maximum estimated Pb-16Li velocity was estimated to be up to 2.9 cm/s (average velocity along the sample is 1 cm/s) in temperature range from 270 to 473  $^{\circ}\text{C}$  [13]. Given the relatively short exposure time, 620 h, the formation of the rough surface documented in Fig. 3 can be classified as early corrosion attack. EDS-line scan revealed minor depletion in Cr content in close neighborhood of interface between resin and steel, as shown in Fig. 4. Decrease in Cr was also reported in Ref. [20]. It is presumed that Cr drop is attributed to higher solubility of Cr in Pb-16Li compared to Fe supporting the model of dissolution mechanism corrosion attack.

Short cracks were recognized on the surface of Fe-Al layer produced

by ECX method, as shown in Fig. 5. It can be assumed that brittleness of coatings likely facilitated the surface crack initiation when exposed to thermal cycles accompanied by solidification and re-melting of the surrounding liquid Pb-16Li during the experimental campaign. A closer inspection of transverse cross-sections revealed formation of large pores dominantly located at the interface between the outer and the diffusion layer. Formation of such pores attributed to Kirkendall effect was previously reported on freshly prepared samples [4]. Reduction of pores in the as-produced diffusion coating was reached through optimized heat treatment [5]. Provided the specimen delivered was almost free of pores, it can be hypothesized that they grew as a result of inter-diffusion processes at the elevated temperature as documented in Fig. 5, where the interface of the coating layers of post irradiated specimen was decorated by large pores. However, these pores may grow or newly form by imbalanced element diffusion, especially of Al at elevated temperature. The number of large pores was found to dominate at higher temperature (see Fig. 5a and c).

All samples coated with the PLD technique were found to be in a pristine condition. It indicates much longer exposure time would be needed to develop some defects. PLD coatings of two different thicknesses have been subject of the scrutiny in terms of corrosion resistance exposed to stagnant Pb-16Li at 550  $^{\circ}\text{C}$  for different time period, as reported in Refs. [18] and [21].

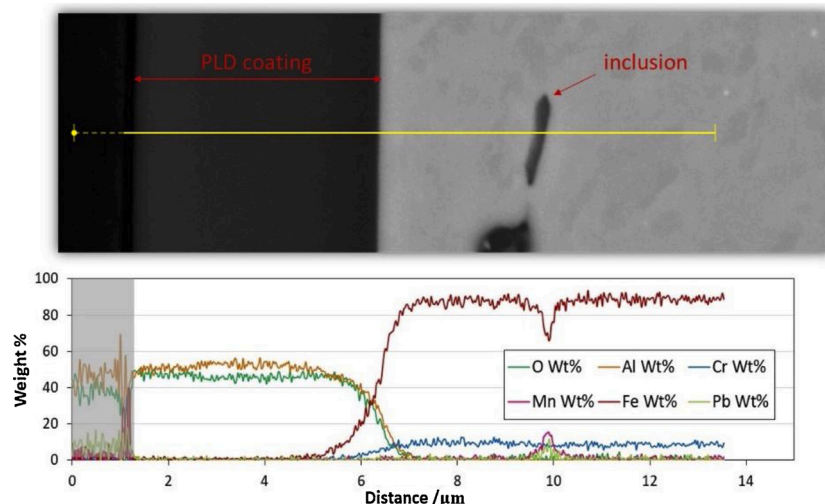


Fig. 9. Line scan of chemical composition of the sample with PLD coating thickness of 5  $\mu\text{m}$ . The signal captured from the resin is marked as a grey region.

## 5. Conclusions

Post-irradiation characterization of the reference and coated tube samples immersed in Pb-16Li and exposed in the LVR-15 reactor campaign for 620 h at 300–425 °C was carried out. Accordingly, the following conclusions can be drawn.

- Formation of rough surface relief was identified as the common aspect of uncoated samples.
- The ECX coating typically appeared with small cracks developed on the surface. The defects in the ECX coating are harder to control and the difficulties to attribute to changes caused by the experiment. Internal pores and voids were found to decorate the interface between outer layer and diffusion layer. The base material is intact with no signs of corrosion attack.
- The PLD coated samples exhibited smooth and intact surface layer. The experiment did not lead to any loss of adhesion or delamination effects at the coating-sample surface interface.

This study was carried out in a close relation to the experimental assessment of tritium permeation reduction factor of the respective coatings. The essential requirement for high permeation reduction is a continuous non-damaged coating layer. Short crack formation or peeling off the coating significantly affects the permeation rate and thus differs from the actual value of respective coating without any damage introduced. In accord to our post irradiation evaluation, no significant damage has been observed reflecting the promising potential of the coating barriers tested.

## Declaration of Competing Interest

The authors report no declarations of interest.

## Acknowledgements

This work has been carried out within the framework of the EUROfusion Consortium and has received funding from the Euratom research and training program 2014-2018 and 2019-2020 under grant agreement No 633053. The views and opinions expressed herein do not necessarily reflect those of the European Commission.

This work has been also supported by the grant no. MSMT-41274/2014-2 from the Ministry of Education, Youth and Sports of the Czech Republic.

## References

- [1] L.V. Boccaccini, G. Aiello, J. Aubert, et al., Objectives and status of EUROfusion DEMO blanket studies, *Fusion Eng. Des.* 109-111 (2016) 1199–1206, <https://doi.org/10.1016/j.fusengdes.2015.12.054>.
- [2] M. Utili, S. Bassini, L. Boccaccini, et al., Status of Pb-16Li technologies for European DEMO fusion reactor, *Fusion Eng. Des.* 146 (2019) 2676–2681, <https://doi.org/10.1016/j.fusengdes.2019.04.083>.
- [3] F. Cisondi, et al., Progress in EU breeding blanket design and integration, *Fusion Eng. Des.* 136 (2018) 782–792, <https://doi.org/10.1016/j.fusengdes.2018.04.009>.
- [4] G. Federici, C. Bachmann, W. Biel, et al., Overview of the design approach and prioritization of R&D activities towards an EU DEMO, *Fusion Eng. Des.* 109-111 (2016) 1464–1474, <https://doi.org/10.1016/j.fusengdes.2015.11.050>.
- [5] J. Konys, W. Krauss, N. Holstein, J. Lorenz, S.E. Wulf, K. Bhanumurthy, Impact of heat treatment on surface chemistry of Al-coated Eurofer for application as anti-corrosion and T-permeation barriers in a flowing Pb–15.7Li environment, *Fusion Eng. Des.* 87 (7-8) (2012) 1483–1486, <https://doi.org/10.1016/j.fusengdes.2012.03.042>.
- [6] S.E. Wulf, W. Krauss, J. Konys, Corrosion resistance of Al-based coatings in flowing Pb–15.7Li produced by aluminum electrodeposition from ionic liquids, *Nucl. Mater. Energy* 9 (2016) 519–523, <https://doi.org/10.1016/j.nme.2016.03.008>.
- [7] S.E. Wulf, W. Krauss, J. Konys, Long-term corrosion behavior of Al-based coatings in flowing Pb–15.7Li, produced by electrochemical ECX process, *Nucl. Mater. Energy* 16 (2018) 158–162, <https://doi.org/10.1016/j.nme.2018.06.019>.
- [8] D. Iadicicco, S. Bassini, M. Vanazzi, et al., Efficient hydrogen and deuterium permeation reduction in Al<sub>2</sub>O<sub>3</sub> coatings with enhanced radiation tolerance and corrosion resistance, *Nucl. Eng. Des.* 312 (2018) 126007, <https://doi.org/10.1088/1741-4326/aadd1d>.
- [9] F.G. Ferré, M. Ormellesse, F. Di Fonzo, M.G. Beghi, Advanced Al<sub>2</sub>O<sub>3</sub> coatings for high temperature operation of steels in heavy liquid metals: a preliminary study, *Corros. Sci.* 77 (2013) 375–378, <https://doi.org/10.1016/j.corsci.2013.07.039>.
- [10] F.G. Ferré, A. Mairo, D. Iadicicco, et al., Corrosion and radiation resistant nanoceramic coatings for lead fast reactors, *Corros. Sci.* 124 (2017) 80–92, <https://doi.org/10.1016/j.corsci.2017.05.011>.
- [11] F.G. Ferré, E. Bertarelli, A. Chiodoni, et al., The mechanical properties of a nanocrystalline Al<sub>2</sub>O<sub>3</sub>/a-Al<sub>2</sub>O<sub>3</sub> composite coating measured by nanoindentation and Brillouin spectroscopy, *Acta Mater.* 61 (7) (2013) 2662–2670, <https://doi.org/10.1016/j.actamat.2013.01.050>.
- [12] S.E. Wulf, N. Holstein, W. Krauss, J. Konys, Influence of deposition conditions on the microstructure of Al-based coatings for applications as corrosion and anti-permeation barrier, *Fusion Eng. Des.* 88 (9-10) (2013) 2530–2534, <https://doi.org/10.1016/j.fusengdes.2013.05.060>.
- [13] E. Gaganidze, F. Gillemot, I. Szenthe, M. Gorley, M. Rieth, E. Diegele, Development of EUROFER97 database and material property handbook, *Fusion Eng. Des.* 135 (2018) 9–14, <https://doi.org/10.1016/j.fusengdes.2018.06.027>.
- [14] F. Di Fonzo, D. Tonini, A. Li Bassi, et al., Growth regimes in pulsed laser deposition of aluminum oxide films, *Appl. Phys. A* 93 (2008) 765–769, <https://doi.org/10.1007/s00339-008-4720-y>.
- [15] E.J. Frankberg, J. Kalikka, F.G. Ferré, et al., Highly ductile amorphous oxide at room temperature and high strain rate, *Science* (New York, N.Y.) 366 (2019) 864–869, <https://doi.org/10.1126/science.aav1254>.
- [16] L. Vála, M. Kordač, T. Melichar, M. Utili, Numerical analyses for conceptual design of an irradiation PbLi capsule for testing of protective coatings for the European DEMO breeding blanket project, *Fusion Eng. Des.* 136 (2018) 797–802, <https://doi.org/10.1016/j.fusengdes.2018.04.011>.
- [17] I.F. Berceruelo, D. Rapisarda, I. Palermo, et al., Thermal-hydraulic design of a DCLL breeding blanket for the EU DEMO, *Fusion Eng. Des.* 124 (2017) 822–826, <https://doi.org/10.1016/j.fusengdes.2017.03.108>.
- [18] M.C. Gasquez, S. Bassini, T. Hernandez, M. Utili, Al<sub>2</sub>O<sub>3</sub> coating as barrier against corrosion in Pb-17Li, *Fusion Eng. Des.* 124 (2017) 837–840, <https://doi.org/10.1016/j.fusengdes.2017.03.070>.
- [19] J. Konys, W. Krauss, J. Novotny, H. Steiner, Z. Voss, O. Wedemeyer, Compatibility behavior of EUROFER steel in flowing Pb–17Li, *J. Nucl. Mater.* 386-388 (2009) 678–681, <https://doi.org/10.1016/j.jnucmat.2008.12.271>.
- [20] M.G. Barker, T. Sample, The solubilities of nickel, manganese and chromium in Pb-17Li, *Fusion Eng. Des.* 14 (3-4) (1991) 219–226, [https://doi.org/10.1016/0920-3796\(91\)90005-B](https://doi.org/10.1016/0920-3796(91)90005-B).
- [21] D. Iadicicco, M. Vanazzi, F.G. Ferré, B. Paladino, S. Bassini, M. Utili, F. Di Fonzo, Multifunctional nanoceramic coatings for future generation nuclear systems, *Fusion Eng. Des.* 146 (2019) 1628–1632, <https://doi.org/10.1016/j.fusengdes.2019.03.004>.